

Full Length Research Paper

Cell growth curves for different cell lines and their relationship with biological activities

Iloki Assanga, S. B.*, Gil-Salido, A. A., Lewis Luján, L. M., Rosas-Durazo, A., Acosta-Silva, A. L., Rivera-Castañeda, E. G. and Rubio-Pino, J. L.

Rubio Pharma y Asociados S. A de C. V., Laboratorio de Investigaciones en Bioactivos y Alimentos Funcionales (LIBAF), Hermosillo, Sonora, México.

Accepted 13 August, 2013

The cellular-growth curves for distinct cell lines (tumor and non-tumor) were established, evaluating the population of doubling time (DT) and maximum growth rate (μ_{max}). These curves define the growth characteristics for each cell line; they allow determination of the best time range for evaluating the effects of some biological compounds. Subsequently, the biological activities of three ethanolic extracts of *Phoradendron californicum* were evaluated in these cells lines; two extracts were of *Prosopis laevigata* (Mesquite tree) from two distinct geographic zones, and the other one was of *Quercus ilex* (Encino/Oak tree). We also evaluated the cytotoxic activity and nitric oxide (NO) scavenging ability of these extracts. The results showed the RAW 264.7 cell-line had the highest growth rate in all experiments. For the rest of cell-lines, we found μ_{max} in the following order: L929 > A549 > ARPE-19 \geq 22Rv1; while the DT was in the order: RAW 264.7 > A549 \geq L929 > ARPE-19 > 22Rv1. With respect to the anti-proliferative activity of the *P. californicum* ethanolic extracts, we observed that the most sensitive cell line was RAW 264.7 (with all three extracts), and the least sensitive was the ARPE-19 cell line; the first one was the fastest growing and the second was the one of the slowest. The anti-oxidative studies by NO scavenging were evaluated in RAW 264.7 cell-line, the best extracts were the ethanolic extracts of *P. californicum* from *P. laevigata* and were geographic zone no-dependent for these biological activities.

Key words: Cellular-growth curve, doubling time (DT), *P. californicum*, anti-proliferative, NO scavenging.

INTRODUCTION

Current cell-culture techniques allow good control of the cellular environment, since the nutrient content concentrations are known which regulate physicochemical and physiological parameters of cell growth (Molina et al., 2004). Cellular culture allows the study of the relationship between host cells and intracellular microorganisms, the analysis of immunological parameters such as cytokines and other proteins, the evaluation of antimicrobial effectiveness, and the performance of cytotoxic assays (evaluation of the effects of drugs or other agents on cancer cells). Methods are available which permit the measure-

ment of viability and proliferation in cell cultures. These methods can be used as a monitoring tool to determine if a sample stimulates, inhibits and/or affects cell growth and viability. One of these methods involves use of the dye Trypan Blue (TB) (Rodriguez et al., 1997), which penetrates dead cell membranes with a blue characteristic color; whereas, the living cells are not dyed with TB and can be counted by hemocytometer under an optical microscope. Another widely applied method is the colorimetric assay [3-(4,5-dimethylthiazol-2-yl)-2,5-diphenyl-tetrazolium bromide] (MTT), which is based on the

*Corresponding author. E-mail: ilokiasb@yahoo.com, drsimoniloki@rubiopharma.com. Tel: 01(662) 236-01-01. Fax: 01(662) 218-48-40.

reduction of MTT to formazan, which has a characteristic purple color. This conversion reflects the enzymatic activity in viable cells, and the dye intensity is proportional to the number of living cells (Mossman, 1983).

The cell-line growth curves are applied in the evaluation of the characteristics of cellular growth, which immediately after reseeding shows a “lag-phase”. The duration of this phase could take from a few hours up to 48 h, the time required for a cell to recover from the trypsinization, to rebuild its cytoskeleton, and to secrete an extracellular matrix that facilitates the linkage between the cells and their propagation along the substrate. All these achievements enable the cell to enter into a new cycle.

Subsequently, the cell enter into exponential growth, “log-phase”, in which the cell population doubles at a characteristic rate defined as DT (characteristic for each cell line), and also the μ_{\max} value can be defined. In this phase, the effects of drugs and chemical agents that stimulate or inhibit cell growth can be studied, as well as the immunomodulatory and radical-scavenging effects of these agents. Finally, when the cell population is very dense and the substrate has practically all been metabolized, the cells enter in a stationary phase, where the rate growth drops nearly to zero (Freshney, 2006).

Some substances, drugs and/or chemical agents are extracted from distinct plant species as bioactive compounds which possess a remarkable biological activity (including medicinal properties), and they are widely applied and studied in complementary and alternative medicine versus diseases as cancer, allergies and diabetes (Kwon et al., 2010). Generally, plants synthesize two mainly metabolic groups in their metabolic phases: primary (essential) and secondary (non-essentials). The first type can be found in high concentrations (amino acids, proteins, carbohydrates, nucleic acids and lipids). On the other hand, the secondary metabolites originate from bioconversion of primary metabolites, and can be found in lesser quantities in plants; they fall into three main categories: terpenes, phenols and nitrogenated compounds (alkaloids) which have been proven to be bioactive compounds with remarkable medicinal properties (Ortiz, 2010; Rivero, 2010; Avalos and Pérez-Urria, 2009). The most important phenolic class is the flavonoids, which are found mainly in vegetables, fruits, grains, barks, roots, flowers, teas and wines. Their most studied and described property is their antioxidant capacity (Nijveldt et al., 2001). The flavonoid groups are defined as compounds with capacities to delay, inhibit and pre-vent oxidation of oxidizable compounds by means of free radical scavenging, thereby diminishing the oxidative stress. Dai and Mumper (2010) define oxidative stress as an unbalanced state characterized by an excessive quantity of reactive oxygen and/or nitrogen species (for example, superoxide anion, hydrogen peroxide, hydroxyl radical, peroxy nitrite and nitric oxide).

NO is an important bio-regulator molecule which has important physiological effects, including blood pressure

control, neuronal signal transduction, modulation of platelet function, and antimicrobial activity, as well as anti-tumor activity. Many of these effects are seen at quite low concentrations of NO. Exposure to bacterial toxins such as lipopolysaccharides stimulates an inflammatory cellular response that releases such factors as nitric oxide, prostaglandin E₂, cytokines, tumor necrosis factor- α and eicosanoid mediators. The NO in macrophages is produced by the inducible form of nitric oxide synthase (iNOS), whose activation causes production of nitric oxide in high concentrations (Chen et al., 2001). During infection and inflammation processes, the NO formation by iNOS can be excessive, causing some undesired deleterious effects (Jagetia et al., 2004; Marcocci et al., 1994a, b; Chen et al., 2001). There are some reports about the biological activity of *P. californicum* (known in United States as “dessert mistletoe” and “toji” in México).

This plant is a very common autotrophic hemiparasite surviving at the expense of its higher vascular plants hosts (Kuijt, 1969; Holland et al., 1977; Calder and Bernhardt, 1983; Ehleringer et al., 1985, 1986). Branches of these host plants often swell during infection by this leafy mistletoe (Holland et al., 1977). *P. californicum* taps its host's xylem, obtaining only water and nutrient mine-rals nutrients from xylem fluids (Leonard and Hull, 1965; Raven, 1983; Ehleringer et al., 1986; Holland et al., 1977).

The aim of this study was to determine the growth curves for several cell lines, characterizing their DT and μ_{\max} , using two methods which we compared. We then studied the impact of *P. californicum* ethanolic extracts from *P. laevigata* and *Q. ilex* on these cellular growth characteristics.

MATERIALS AND METHODS

Cell culture

The following cell lines were used: L929 (mouse, subcutaneous connective tissue), A549 (human caucasian lung carcinoma), NCI-H1395 (human lung adenocarcinoma), 22Rv1 (human prostate carcinoma) and RAW 264.7 (mouse leukaemic monocyte macrophage cell line), all were obtained from the American Type Culture Collection (ATCC). The ARPE-19 (non-tumoral human retina) line was donated by Horacio L. Rilo, MD (University of Arizona). All adherent cellular lines were cultured in bottles of 25 cm³ from corning with Dulbecco's Modified Eagle's Medium (DMEM) at 7.2 to 7.4 pH. The medium was supplied at 5% with fetal bovine serum (FBS); only the line ARPE-19 was supplied at 10% FBS, the rest of the supplements were penicillin/streptomycin (1%), glutamine (0.75%) and sodium pyruvate (1%). The medium and all the supplements were obtained from Sigma-Aldrich. The culture was sterilized by filtration with filter Millipore membranes pore size of 0.45 μm . All the culture bottles with the cellular lines were maintained in a 5% CO₂ flux incubator (Binder) at 37 °C.

Plant material: Collection

Stem of Mesquite was collected in middle-west and north-west region of Sonora (Tazajal, City), and the *P. Californicum* of Encino was collected in north-west Sonora (Carbo, City), Mexico in 2009 to

2010. The aerial parts of the plant were dried at room temperature for 15 days. Samples were ground and packed until analysis.

Extracts preparation

Stems of *P. californicum* from Mesquite and Encino trees were extracted by maceration with ethanol solvent in Erlenmeyer flasks during 7 to 10 days at room temperature. Three continuous extraction processes were carried out. All extracts were filtered and the filtrates were concentrated with a vacuum rotary evaporator (Buchi) at 36°C. The ethanolic extracts were stored at 4°C until they were used.

Cell-growth curves

Once the cell-lines reached 80 to 90% of confluence, they were counted in a Neubauer camera at 1:2 dilution with trypan blue dye exclusion (purchased from SIGMA-Aldrich). The cells were plated at a density of 2,500 cells per well in a 96 well plate to determine the proliferation parameters by the MTT method (described in MTT Assays). On the other hand, to determine the cell number parameter, the cells were seeded at a density of 20,000 cells per well in a corning 12 well plate (22.1 mm of diameter) and the counts were performed in a Neubauer camera by TB dye exclusion. Both determinations were carried out for 24 h for 17 days, and the medium was replaced each 3 days. The μ_{max} for each cellular line was determined by a non-linear regression curves analysis (Ramírez and Molina, 2005). The quantification of DT as a measure of cell growth for each cell line has been carried out using either the counting of total viable cells (haemocytometer chambers) or colorimetric assay (as described in the MTT Assays).

Preliminary phytochemical screening

Phytochemical screening (Alhassan et al., 2009) of the extracts were carried out to identify the secondary metabolites such as alkaloids (Mayer's and Draggendorff's test), carotenes (Carr-Price test), triterpens/steroids (Liebermann-Burchard test), lactone groups (Baljet test), lipids and essentials oils (Sudan III test), reducing compounds (Fehling test), flavonoids (Shinona test), saponins (Frothing test) and anthraquinones (Borntrager's test) according to standard phytochemical methods as described by Chhabra et al. (1984).

MTT assay: Anti-proliferative assays

The assays were carried out adding 10 μ L of MTT [3-(4,5-dimethylthiazol-2-yl)-2,5-diphenyltetrazolium bromide] (obtained from SIGMA-Aldrich) solution (5 mg/ml) for each well, then incubating for 4 h. Formed formazan crystals were dissolved with 100 μ L of isopropyl alcohol at 0.05 N HCl, and the absorbance measures were registered at 570 nm on a micro-plate reader (Thermo Scientific Multiskan Spectrum) using the wavelength of 655 nm as reference (Mossman, 1983), the data results were processed on a SkanIt Software 2.4.2. To determine the anti-proliferative activity for the different extracts, the cell-lines were seeded (per triplicates) at a density of 10×10^4 cells/well (50 μ L) in 96 well plates, and allowed to adhere during 24 h at 37°C with 5% of CO₂ and 95% of relative humidity. After 24 h of pre-incubation, 50 μ L of the sample-extracts were added at distinct concentrations to the cell-lines, and the period of incubation continued for another 48 h. All assays were carried out in the "log" cellular-growing phase. The percentage inhibition of proliferation was calculated comparing the absorbance values of the control (cell line without sample-extracts) and the test samples.

The anti-proliferative activity of the extract was expressed as IC-50; and the cytotoxic selectivity index (SI) was calculated using the formula: IC-50 of extract in a no tumoral cell line/IC-50 of extract in a tumor cell line, where IC-50 is the concentration required to kill 50% of the cell population (Badisa et al., 2009).

Nitric oxide (NO) determination

The RAW 264.7 cell-line in the "log-phase" of growth was activated with lipopolysaccharide (LPS) according to the previous study of Kim et al. (1999). First, the RAW 264.7 cells were plated in 96-well plates (2×10^5 cells/well) and pre-incubated for 24 h. After the pre-incubation, LPS 1 μ g/ml was added to the cells sample, and was incubated 4 h more. The sample-extracts were dissolved in dimethyl sulfoxide (DMSO; from SIGMA-Aldrich) and diluted with DMEM supplied at 5% FBS into appropriate concentrations, and incubated for another 48 h. 1 mM of *N*_ω-Nitro-L-arginine methyl ester hydrochloride (L-NAME hydrochloride) (obtained from SIGMA-Aldrich) was used as suppressor of the inducible nitric oxide synthase (iNOS) enzyme. The concentration of nitrite NO₂⁻, the stable conversion product of NO, was determined using the Griess reagent [1:1 mixture (v/v) of 1% sulfanilamide (in 60% of acetic acid) and 0.1% *N*-(1-Naphthyl)ethylenediamine dihydrochloride, both reagents were purchased from SIGMA-Aldrich, and the optical density data were recorded at 550 nm in a micro-plate reader.

A standard curve of sodium nitrite was used to find the concentrations of nitrites produced by the RAW cells (Griess method). The absorbance measures were realized on a micro-plate reader (Thermo Scientific Multiskan Spectrum) and the data results were processed on a SkanIt Software 2.4.2.

Statistical analysis

All measurements were carried out by triplicate in three different replicates. The data results of the growth curve were normalized at logarithmic scale. On the other hand, the growth curve of RAW 264.7 line was modeled by non-linear polynomial fitting. The results were analyzed based on variance analysis (ANOVA). Significant differences between means were determined by Tukey test with 95% of confidence. All the analytical features were determined in Origin Pro-2008 program.

RESULTS AND DISCUSSION

Figure 1 depicts the cellular-growth curves for tumor and no-tumor cellular lines determined by TB (Figure 1a) and MTT (Figure 1b) assays. In Figure 1a, it is possible to appreciate that after the first 50 h of incubation, the cellular growth begins in an exponential fashion in practically all cell lines. RAW 264.7 line shows the highest growth rate in this experiment; whereas the growth rates of the rest of the cellular lines were as follows: RAW 264.7 > A549 > L929 > 22Rv1 ≥ ARPE-19 > NCI-H1395. Only the RAW 264.7 line manifested four phases of cell growth, while the rest of cell lines only manifest the "lag and log-phases". In the specific case of NCI-H1395 line, this one never reaches the "log-phase", as it remains practically on the "lag-phase"; actually, the 22Rv1, ARPE-19 and NCI-H1395 lines are classified as "slow growth cell lines". It is important to indicate that L929, ARPE-19 and 22Rv1 lines show remarkable decays in their number

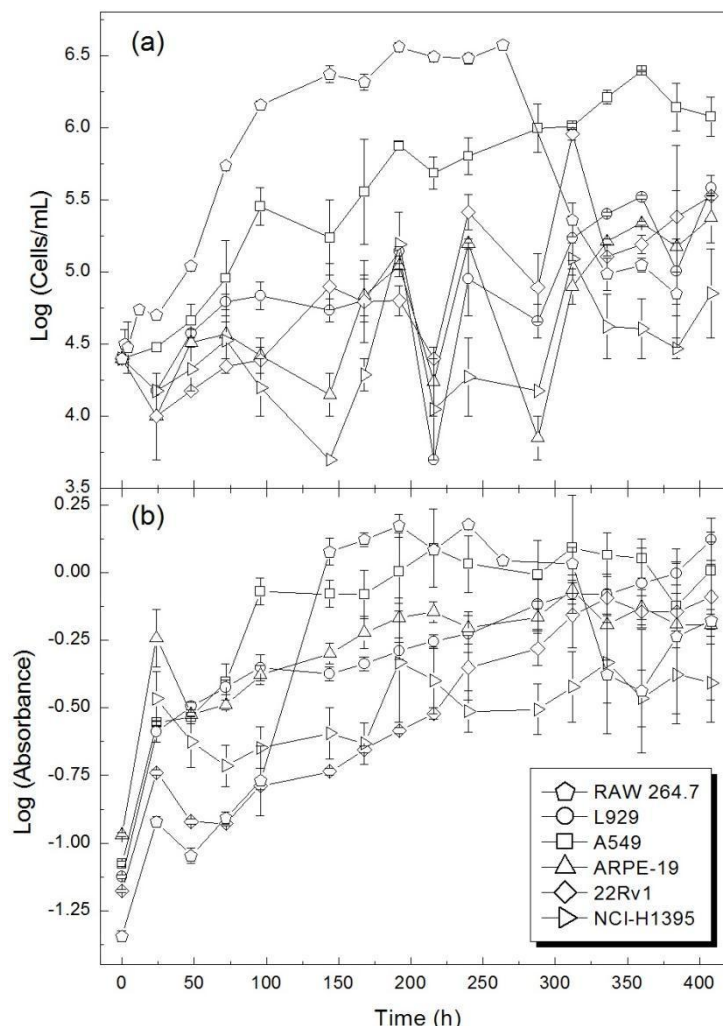


Figure 1. Cellular-growth curves determined by TB (counting dye method) and MTT (optical density method) correspond to Figure 1a and 1b respectively). All measures were performed per triplicate.

of cells at 216 and 288 h of running times. This behavior cannot be appreciated in the cellular-growth curve determined by MTT assays (Figure 1b). A possible interpretation of these behaviors is the relative subjectivity of visual cell counting with the TB exclusion method (Figure 1a). In addition, the standard deviations of trypan blue counts were usually larger than those for optical density in the MTT assay. Nonetheless, this TB method has some advantages over measurement of absorbance on spectrophotometers – the main ones being its utility for observation of cell morphology and detection of culture contaminants. This test is simple and inexpensive; it provides a rapid method for assessing cell viability and allows comparison of suspension homogeneity (Candurra et al., 1994; Graves et al., 2006; Lu et al., 2009).

In the case of Figure 1b, the “lag-phase” is present in all cellular lines during the first 72 h of incubation. After

this period, the “log-phase” starts to indicate that the growth is more remarkable for RAW 264.7 and A549 lines than the rest of cellular lines. In the RAW 264.7 line, the four typical cellular growth phases are noticeable, in accord with what we observed in TB assays (Figure 1a); these results indicate a good correlation between these methods. Conversely, the rest of the cellular lines characterized by MTT assays only manifest the “lag and log-phases”, except for the NCI-H1395 line which never reaches an evident “log-phase”. Therefore, the cellular-growth curve characterized by MTT method is as follows: RAW 264.7 > A549 > L929 ≥ ARPE-19 > 22Rv1 > NCI-H1395. On the other hand, Table 1 shows the ω_{max} determined values for each cell line (Ramírez and Molina, 2005) by both methods (TB and MTT assays). It is possible to observe that the obtained ω_{max} values are similar with both methods; although, the values calculated

Table 1. Comparison between the μ_{\max} values for the distinct cell-lines determined by MTT and TB methods.

Cell-Line	t (h)	μ_{\max} (h^{-1})	
		MTT	TB
RAW 264.7	144	0.0249	0.0337
L929	120	0.0139	0.0149
A549	216	0.0105	0.0172
ARPE-19	216	0.0070	ND
22Rv1	336	0.0068	0.0123
NCI-H1395	---	ND	ND

ND: No detected

with the TB method were incrementally higher for each cell line. The time at which their ω_{\max} values are reached is a distinct characteristic of each cell-line. The RAW 264.7 line shows the highest ω_{\max} value at 144 h; whereas, the 22Rv1 line has the lowest ω_{\max} value. Moreover, the ω_{\max} parameter shows a descending order as follows: RAW 264.7 > L929 > A549 > ARPE-19 \geq 22Rv1. It should be noted that the NCI-H1395 line never reaches a consistent ω_{\max} value, since it never reaches its "log-phase" of growth.

Figure 2 shows the UV lambda scattering spectra at distinct run-times for cellular-growth curves presented in Figure 1b. First, it is important to note that the behavior of the distinct cellular-lines in panel 2a show that the number of cells at 24 h continues being minimal; therefore, the spectrum values do not show significant differences between them. A detailed inspection of the rest of the panels (Figure 2b to d) confirms an exponential growth for all cellular-lines. In the panel 3c, the assay middle run times are represented for all cellular-lines, which denotes a wide difference between the RAW 264.7 line spectrum intensity with respect to the rest of cellular-lines. The panels 2b and c correspond to 120 and 288 h of run times, respectively; a clear tendency of the cellular growth could be appreciated as follows: RAW 264.7 > A549 > L929 \geq ARPE-19 > 22Rv1 > NCI-H1395. The A549 line maintains practically the same absorbance values in panels 2d (408 h) and c; however, in the case of the RAW 264.7 line, a remarkable drop in its absorbance values is observed; whereas, the L929 line reflects an important increment as corroborated in Figure 1b. All panels (2a to d) show the maximum absorbance behavior at 570 nm for all cellular lines where this absorbance increases through time. These differences between spectra could be due to the characteristic values of growth rate (ω_{\max}) and the amount of metabolized MTT for each cell line. Some lines are less efficient MTT metabolizers, as in the case of the human cell lines (Scudiero et al., 1988). The human cell line NCI-H1395 was the slowest converter of MTT to formazan; whereas, the L929 murine line was the fastest.

In the Figure 3, the cellular growth curves for the RAW 264.7 and A549 lines were modeled by means of polynomial non-linear regression and correspond to Figures 1a and b (TB and MTT assays, respectively). The overall models are significant, and we can achieve a seventh and third polynomials order with a high fit model ($R^2 > 0.90$). Figures 3a (TB) and 3c (MTT) show the cellular growth curves for RAW 264.7 line, which manifest all characteristic cellular growth phases. The behavior of the curves in the Figure 3a is as follows: "lag-phase" (0 to 24 h), "log-phase" (24 to 192 h), "plateau-phase" (192 to 264 h) and "decay-phase" (264 to 384 h). On the other hand, the growth curve behavior in the Figure 3c shows some differences in its phases in relation to the Figure 3a except in the "lag-phase" which is identical for both curves; the rest of the phases have a behavior as follows:

"Log-phase" (24 to 144 h), "plateau-phase" (144 to 312 h) and "decay-phase" (312 to 384 h), in which the "decay-phase" is less sharp than the one depicted in Figure 3a. It should be noted that both curves were adjusted by means of polynomial model order 7. As far as the modeling of the curve for the A549 line determined by TB method (Figure 3b), it confirms only two cellular-growth phases: "Lag-phase" (0 to 24 h) and the "log-phase" (24 to 408 h), corresponding to what is observed in Figure 1a where the "log-phase" continues until the experiment ended at 408 h; while by the MTT method (Figure 3d), the three growing phases the "lag-phase" (0 to 24 h), the "log-phase" (24 to 216 h) and the "plateau-phase" (216 to 408 h) can be appreciated as observed in the Figure 1b. The polynomial models applied to the adjustment of the curves by TB and MTT methods are in the order 3 and 5, respectively. In spite of the existence of small differences between both methods, the polynomial model is maintained with a good adjustment value. Meanwhile, by these mathematic models, it is theoretically possible to confirm the cellular growth behavior for these two counting cellular methods.

Figure 4 represents the results of DT data for the distinct cellular lines obtained by TB and MTT assays. A detailed inspection of the results reveals similar growth patterns for the RAW 264.7, A549, L929 and ARPE-19 lines by both methods. On the other hand, the 22Rv1 line shows DT values that differ between TB (63 h) and MTT (94 h) methods; this could be due to the physiological characteristics inherent in each cellular line, because during dilution preparations for cellular counting assays some clusters were found, which made the observations difficult, entailing a significantly experimental error with the TB assay in relation to the MTT assay. Generally, the DT result could depend on three main factors: 1) cellular system type in culture (tumor versus non-tumor); 2) type of tissue; and 3) the species of origin (Scudiero et al., 1988; Rodriguez et al., 1997). Some authors have reported DT determinations for distinct cellular lines. One of these was carried out by He et al. (2001); they found a DT value for the A549 line of 23.5 h, while Graves et al. (2006) reported a DT value of 22.3 h. Both researchers

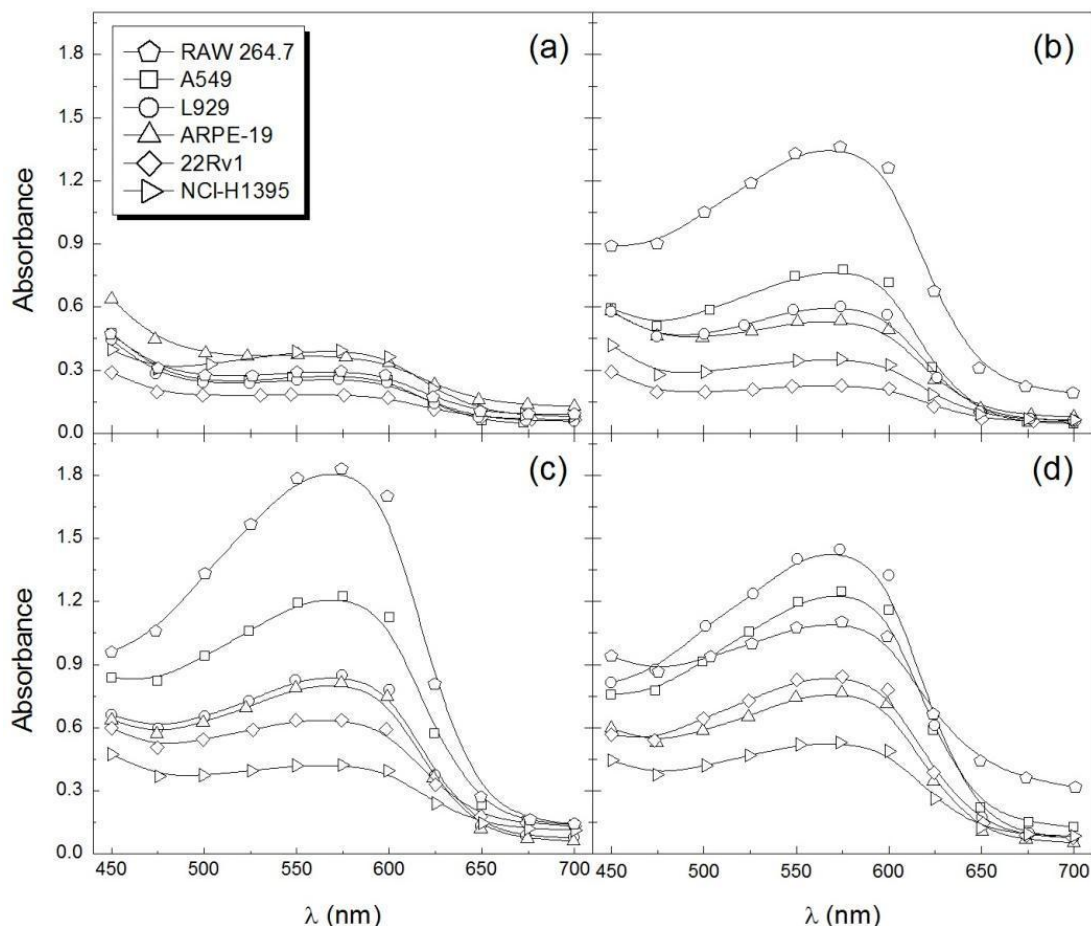


Figure 2. Sweep-lambda UV-absorption spectra of MTT metabolized for each cell-line corresponding to Figure 1b at distinct growth times. Panels: (a) 24 h; (b) 120 h; (c) 288 h and (d) 408 h.

cultured their cellular lines under the same conditions (RPMI-1640 culture-medium supplemented with 10% FBS). However, He et al. (2001) performed the determinations by Coulter counter and Graves used the TB method. In this work, we determined DT values of 27 h for the A549 cell line, which is similar to the DT of 27.29 h reported by Lu et al. (2009) at distinct culture conditions (RPMI-1640, 10% FBS). On the other hand, the DT value reported by ATCC for the same cell line is 22 h, and the culture medium recommended is F-12K supplemented with 10% FBS.

The L929 line registered DT values of 32 and 28 h by MTT and TB assays, respectively. These results were similar to those reported by Baca et al. (1985), where they found a DT value of 33 h and their culture conditions were similar to those employed in this study, in that they used Eagle essential medium supplemented with 5% calf serum. Nevertheless, Wataha et al. (1994) reported a DT of 42 h for the same cell-line, they used F-12 culture medium with 5% FBS. Moreover, the ATCC reported a DT value of 53 h, and they recommended EMEM medium culture with 10% horse serum. For RAW 264.7 line, our

DT values determined were of 11 and 12 h by cell-counting (Trypan blue) and MTT assays, respectively. These results are in accordance with those determined by Sakagami et al. (2009); they obtained a DT value of 11 h, but they used a DMEM culture medium with 10% FBS.

There are few studies cited about the evaluation of DT for ARPE-19, 22Rv1 and NCI-H1395 cell lines. For the ARPE-19 line, DT values of 28.5 ± 5.1 h have been reported, using DMEM culture medium supplemented with 15% FBS (Tezel et al., 2004). In this study, we found DT values of 55 h by TB assay, and 65 h with the MTT method. The reasons for the discrepancies may be differences in the medium and serum composition, as well as selection for slower growing cells during repeated subculture. For the 22Rv1 line, the ATCC reported a DT value of 40 h, based on studies by Sramkoski et al. (1999), they cultured the cell line with RPMI culture medium at 10% fetal bovine serum and they reported that this cell line grows slowly to a high cell culture density. This result is different than that found in this work, as our cellular counting (TB method) revealed DT values of 63 and 94 h with MTT assay. For the last cell line, NCI-

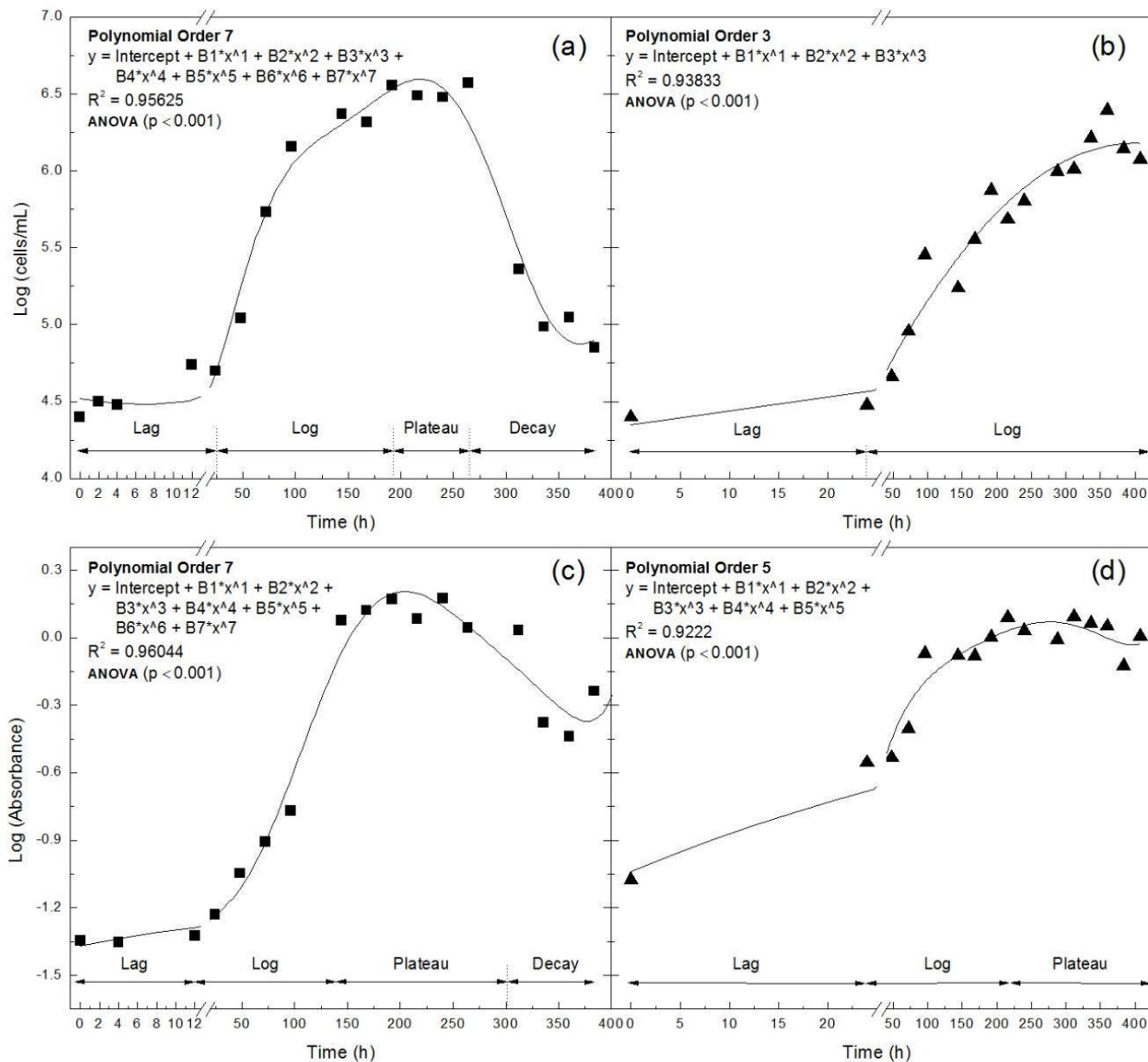


Figure 3. Polynomial models of cellular-growth curves for RAW 264.7 and A549 lines. Panels 3a and 3b denotes the curves determined by TB method for RAW 264.7 and A549 lines respectively. Panels 3c and 3d shows the curves determined by MTT method for RAW 264.7 and A549 lines respectively. On each Panel are needed the polynomial order modeling treatment and the distinct cellular-growth phases.

H1395, it was not possible to calculate its DT, since this line is very slow growing and never reached the “log-phase”, because is a very slow growth cellular line. The precise reasons for why our results for DT values of distinct cell lines differ from those of some other researchers are no clear. Wataha et al. (1994) concluded that differences in the medium and serum compositions, as well as selection of faster growing cells during repeated subculture, are probably responsible. Since *P. californicum* is a poorly studied plant, it is desirable to subject it to a

phytochemical screening. In Table 2, we have denoted the presence or absence of secondary metabolites responsible for the medicinal proprieties of plants. *P. californicum* is a plant rich in flavonoids, saponins, phenols and/or tannins principally; these can often act as antiproliferative and antioxidant compounds (Quideau et al., 2011). In addition to growth curves for the distinct cell-lines, the biological activity of *P. californicum* extracts was evaluated (Table 3). Our extracts were tested in tumor RAW 264.7 and A549 and non-tumor L929 and

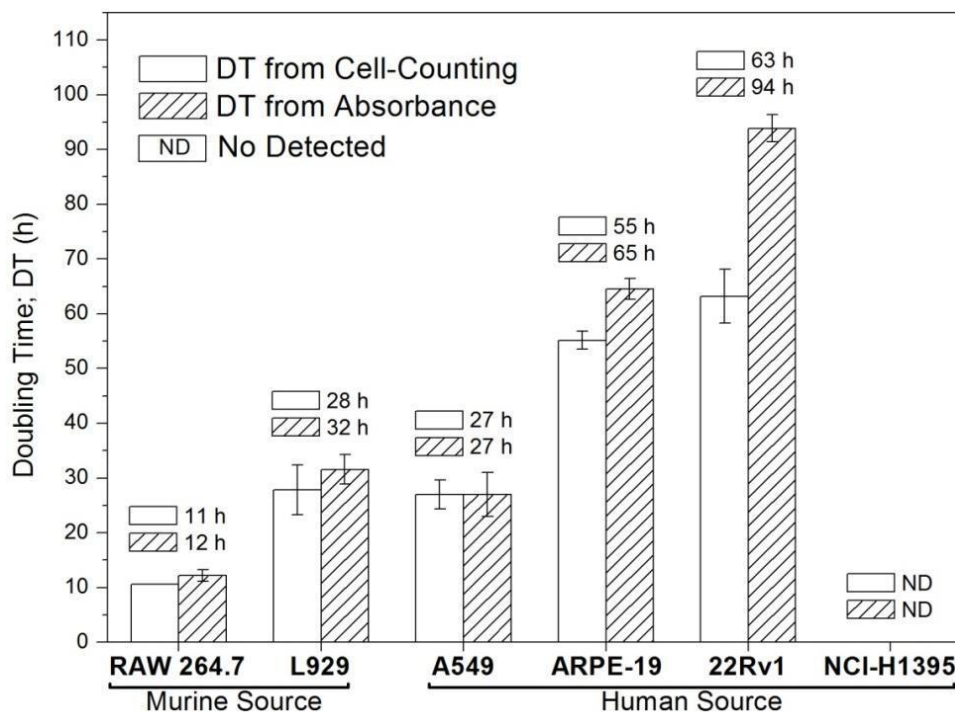


Figure 4. DT parameter determined by TB and MTT methods for the distinct cell-lines.

Table 2. Qualitative Phytochemical Analysis of the ethanolic extract of *P. californicum*.

Phase	(-)	(+)	(++)	(+++)
Methanolic	Lactonic Groups Alkaloids	-	Reducing Compounds Quinones Flavonoids	Saponins Tannins Amines and/or Amino Acids
Aqueous	Alkaloids, Saponins, Phenols and/or Tannins, Reducing Compounds	-		Flavonoids
Hexane	Alkaloids, Quinones, Lipids and/or Essential Oils	Carotenes		Lactonic Groups

-, Absent secondary metabolite; +, Little presence of secondary metabolite; ++, Moderate presence of secondary metabolite; +++, Abundant presence of secondary metabolite.

ARPE-19 cell lines, with the aim to relate their sensitivity to the extracts with their population doubling times; previous research has indicated that shorter DT values tend to be associated with increased sensitivity and increased metabolic rate. We observed that all *P. californicum* extracts exhibited anti-proliferative activity in tumor and non-tumor cellular lines from human and murine sources in a concentration-dependent manner. The IC-50 values determined for all extracts are shown in Table 3.

The *P. californicum* extracts had a more remarkable antiproliferative action on RAW 264.7 and L929 lines than on the ARPE-19 and A549 lines. The RAW 264.7 line, exhibiting the lowest DT value (11 h) was the most sus-

ceptible cell line. The non-tumor cellular line ARPE-19, which showed much less susceptibility to the effects of the extracts than the tumor cellular line A549, actually has the highest DT values (65 h). It is notable that the cell line with lowest DT was most sensitive (RAW 264.7), while the cell line with the highest DT was the least sensitive. Similar patterns with metal ions were documented by Wataha et al. (1994); they observed that short DT values implied increased sensitivity and longer DT values implied decreased sensitivity, in Balb/c and WI-38 cellular lines, respectively. The *P. californicum* from distinct geographic zones displayed a significant difference in the anti-proliferative activity only in the RAW 264.7 line. The chemotherapy agent 5-FU employed as positive control

Table 3. Anti-proliferative activity (IC₅₀)* of the *P. californicum* (Toji) extracts.

Ethanollic xtract	Murin cell line			Human cell line		
	RAW 264.7	L929	SI	A549	ARPE-19	SI
A. Toji-Mesquite	43.49 ± 2.59 ^{A,a}	45.85 ± 23.0 ^{A,a}	1.05	58.5 ± 8.0 ^{A,a}	207.90 ± 23.91 ^{B,a}	3.55
B. Toji-Mesquite	21.06 ± 2.75 ^{A,b}	40.44 ± 6.0 ^{B,a}	1.92	37.52 ± 11.88 ^{A,a}	220.50 ± 28.78 ^{B,a}	5.88
B. Toji-Encino	56.49 ± 0.81 ^{A,c}	42.98 ± 4.25 ^{A,a}	0.82	56.2 ± 6.41 ^{A,a}	354.67 ± 33.94 ^{B,b}	6.31
5- Fluorouracil	270.38/35.1	>1000/130	>3.70	705.12/91.66	>1000/130	>1.42

A, Corresponding to meddle-west region of Sonora (Tazajal Town); B, Corresponding to north-west region of Sonora (Carbo Town); SI, Selectivity Index. Means with different letters in the same column differed significantly ($p < 0.05$), Means with different capital letters in the same row differed significantly ($p < 0.05$) between cell lines from the same source. *IC₅₀ value of extracts ($\mu\text{g/mL}$) or compounds ($\mu\text{M}/\mu\text{g}\cdot\text{mL}$) are representative of at least three independent experiments. All values represent mean of triplicate determination \pm D.E. 5-Fluoracil was used as positive control in the antiproliferative assays.

Table 4. NO scavenging of the *P. californicum* (Toji) extracts.

Ethanollic extract	Tested Extract Concentration			
	12.5 $\mu\text{g/ml}$		25 $\mu\text{g/ml}$	
	% NO Scavenging	% Survival	% NO Scavenging	% Survival
A. Toji-Mesquite	94.19 ± 10.06 ^a	90.4 ± 9.27 ^a	100 ± 0.0 ^a	43.74 ± 5.66 ^a
B. Toji-Mesquite	98.21 ± 3.11 ^a	92.24 ± 2.63 ^a	100 ± 0.0 ^a	82.52 ± 4.98 ^b
B. Toji-Encino	37.07 ± 1.51 ^b	88.94 ± 9.01 ^a	39.62 ± 4.5 ^b	78.59 ± 4.83 ^b
L-name	62.41 ± 4.65 ^c	100 ± 0.0 ^a		

A, Corresponding to meddle-west region of Sonora (Tazajal Town); B, Corresponding to north-west region of Sonora (Carbo Town). Means with different letters in the same column differed significantly ($p < 0.05$). All values represent mean of triplicate determination \pm D.E. The % NO Scavenging and % Survival were tested after 72 h of incubation in RAW 264.7 line; L-NAME was evaluated at 1mM.

The Ethanollic extracts of toji were evaluated at 12.5 and 25 $\mu\text{g/ml}$.

showed the IC-50 values higher than all *P. californicum* extracts. Another important parameter to determine in this kind of study is the selectivity index (SI). In the murine cell lines, only the ethanollic extract of the *P. californicum* (mesquite B) showed the best activity in the RAW 264.7 line, with SI = 1.92. Within the human cell lines, the A549 line was more susceptible to the all extracts evaluated, but the ethanollic extract of the *P. californicum* (mesquite B) was the best, as it had a low IC-50 value (37.52 \pm 11.88) and a high SI value (5.88). With respect to the positive control 5-FU, the murine tumor cellular line was more susceptible than the human tumor cell line, and its SI in the human cell lines was less than that of the extracts evaluated; this indicates that our extracts are more effective for slowing the growth of a human cancer cell line as compared to a non-tumor cell line, and hence may be candidates for use in human cancer therapy.

Table 4 shows the antioxidant activity of Toji-Mesquite and Toji-Encino ethanollic extracts in the RAW 264.7 line. It is important to note that studies were carried out after 72 h of pre-incubation, to insure that the cellular line was in the "log-phase". This was corroborated with the growth curve represented in the Figures 1 and 3. The NO scavenging results between Toji-Mesquite and Toji-Encino

ethanollic extracts differed significantly; the best were obtained with the Toji Mesquite ethanollic extracts, which did not differ between different geographic zones. We also evaluated the effects of the enzymatic inhibitor compound L-NAME as a positive control. This exhibited an important inhibition of the NO production (62.4%) at a concentration of 269.7 $\mu\text{g/ml}$ (1 mM). On the other hand, Toji-Mesquite ethanollic extracts showed a much higher scavenging percentage than the L-NAME at a much lower concentration (12.5 $\mu\text{g/ml}$). Mu et al. (2001) found an inhibition of NO production by the flavonoid quercetin of 22.85% at a concentration of 15 $\mu\text{g/ml}$. In fact, our extracts exhibited a more impressive effect than this flavonoid. Importantly, for all extracts, 12 $\mu\text{g/ml}$ was non-cytotoxic in our cell lines, pointing to a unique anti-inflammatory activity in the extract independent of any effect on cell proliferation or viability. On the other hand, at 25 $\mu\text{g/ml}$, a decrease in cell survival was noted. The cell-growth curves provide valuable information about the cell-number viability at a given time, the subculture frequency and the phase of cell growth. This cell culture characterization allows standardization of physiological and nutritional requirements, enabling improvement of yield and culture conditions (Morgan and Darling, 1995; Candurra et al., 1994; Molina et al., 2004).

The cell-growth curves for distinct cell-lines by Trypan blue (hematocytometer) and MTT methods were performed. The MTT assay was the most efficient, due to less experimental error. Nevertheless, this method has a great disadvantage with respect to Trypan blue, since it does not allow observation of cellular morphology, especially in the cell growth curve. In the literature, there are few studies evaluating cellular-growth curves for several cell-lines, determining DT and ω_{max} . In the present study, it was important to analyze the behaviors of the distinct cell-lines, so that we could evaluate the anti-proliferative effects and the NO scavenging activities of different *P. californicum* ethanolic extracts. The anti-proliferative and NO scavenging activities were evaluated. The susceptibility to growth inhibition with extracts were greater in RAW 264.7 than in L929, likely because the RAW 264.7 line has low DT values and so is a cell line with an accelerated metabolism. In the human cell lines, tumor line A549 was more susceptible than the non-tumor line ARPE-19, concordant with the lower DT A549. It is important to note that regardless of the species, the DT values for L929 and A549 cellular lines are very similar; these results suggest that the tissue of origin is crucial to the cellular growth behavior. On the other hand, the evaluation of percent NO scavenging was performed in "log-phase" of RAW 264.7 line, where we observed the best effects in Toji-Mesquite extracts regardless of their geographical origin.

ACKNOWLEDGEMENT

The authors wish to express their thanks to Dr. Mark F. McCarty, Ph.D San Diego, California, USA for his kindly support in the English revision.

REFERENCES

- Alhassan AJ, Sule MS, Aliyu SA, Aliyu MD (2009). Ideal hepatotoxicity model in rats using carbon tetrachloride (CCl₄). Bayero J. Pure Appl. Sci. 2(2):185-187.
- Ávalos GA, Pérez CU (2009). Metabolismo secundario de plantas. Reduca (Biología). Serie Fisiología Vegetal 2(3):119-145.
- Baca OG, Scott TO, Akporiaye ET, DeBlassie R, Crissman HA (1985). Cell cycle distribution patterns and generation times of L929 fibroblast cell persistently infected with Coxiella burnetii. Infect. Immun. 47(2):366.
- Badisa RB, Darling-Reed S F, Joseph P, Cooperwood JS, Latinwo LM and Goodman CB (2009). Selective Cytotoxic Activities of Two Novel Synthetic Drugs on Human Breast Carcinoma MCF-7 Cells. Anticancer Res. 29(8):2993-2996.
- Calder M, Bernhardt P (1983). The biology of mistletoes. New York, Academic Press.
- Candurra N, Claus J, Coronato S, Coto C (1994). Cultivos celulares y su aplicación en biotecnología. Acta Bioquim. Clín. Latinoam. 2:1-77.
- Chen YC, Shen SC, Lee WR, Hou WC, Yang LL, Lee TJ (2001). Inhibition of nitric oxide synthase inhibitors and lipopolysaccharide induced inducible NOS and cyclooxygenase-2 gene expressions by rutin, quercetin, and quercetin pentaacetate in RAW 264.7 macrophages. J. Cell. Biochem. 82(4):534-548.
- Chhabra SC, Ulso FC, Mshiu EN (1984). Phytochemical screening of Tanzanian medicinal plants. I. J. Ethnopharmacol. 11(2):157-159.
- Ehleringer, JR. Cook CS, Tieszen LL (1986a). Comparative water use and nitrogen relationships in a mistletoe and its host. Oecologia 68(2):279-284.
- Ehleringer JR. Schultz ED (1985). Mineral concentrations in an autoparasitic *Phoradendrom californicum* growing on a parasitic *P. californicum* and its host, *Cercidium floridum*. Am. J. Bot.72(4):568-571.
- Freshney RI (2006). Basic Principles of Cell Culture. Culture Cells for Tissue Engineering. R. I. Freshney. Glasgow, John Wiley & Sons: pp.1-22.
- Graves TG, Harr MW, Crawford EL, Willey JC (2006). Stable low-level expression of p21^{WAF1/CIP1} in A549 human bronchogenic carcinoma cell line-derived clones down-regulates E2F1 mRNA and restores cell proliferation control. Mol. Cancer 5(1):1-13.
- He L, Huang CP, Horwitz SB (2001). Mutations in β -Tubulin map to domains involved in regulation of microtubule stability in Epithelone-resistant cell lines. Mol. Cancer Ther. 1(1): 3-10.
- Holland JS, Grater RK, Huntziger (1977). Flowering plants of the Lake Mead region. Southwest Parks and Monuments Association, Popular Series 23:49.
- Jagetia GC, Rao, SK, Baliga MS, Babu KS (2004). The evaluation of nitric oxide scavenging activity of certain herbal formulations *in vitro*: A preliminary study. Phytother. Res. 18(7):561-565.
- Kim HK, Cheon BS, Kim YH, Kim SY, Kim HP (1999). Effects of naturally occurring flavonoids on nitric oxide production in the macrophage cell line RAW 264.7 and their structure-activity relationships. Biochem. Pharmacol. 58(5):759-765.
- Kuijt J (1969). The biology of parasitic flowering plants. Berkeley, University of California Press.
- Kwon HK, Hwang JS, Lee CG, Sahoo A, Ryu JH, Jeon WK, Ko BS, Im CR, Lee SH, Park ZY, Im SH (2010). Cinnamon extract induces tumor cell death through inhibition of NF κ B and AP1. BMC Cancer 10:392.
- Leonard OA, Hull RJ (1965). Translocation relationships in a between mistletoes and their hosts. Hilgardia 37:115-153.
- Lu ZJ, Ren YQ, Wang GP, Song Q, Li M, Jiang SS, Ning T, Guan YS (2009). Biological behaviors and proteomics analysis of hybrid cell line EAhy926 and its parent cell line A549. J. Experim. Clin. Cancer Res. 28(16):1-10.
- Marcocci L, Maguire JJ, Droy-Lefaix MT, Packer L (1994a). The nitric oxide-savenging properties of *Ginkgo biloba* extract EGb 761. Biochem. Biophys. Res. Commun. 201(2):748-755.
- Marcocci L, Packer L, Droy-Lefaix MT, Sekaki AH, Gardes-Albert M (1994b). Antioxidant action of *Ginkgo biloba* extract EGb 761. Methods Enzym. 234:462-475.
- Molina NB, Minvielle MC, Basualdo JA (2004). Células RK13: Influencia de la concentración de suero fetal bovino en el tiempo de duplicación *." Acta Bioquímica Clínica Latinoamericana 38(4):477-480.
- Morgan DC, Darling SJ (1995). Cultivo de células animales. Zaragoza. Mossman T (1983). Rapid colorimetric assay for cellular growth and survivals: Application of proliferation and cytotoxicity assays. J. Immunol. Methods 65(1-2):55-63. Mu MM, Chakravorty D, Sujiyama T, Koide N, Takahashi K, Mori I, Yoshida T, Yokoshi T (2001). The inhibitory action of quercetin on lipopolysaccharide- induced nitric oxide production in RAW 264.7 macrophages cells. J. Endotoxin Res. 7(6):431-438.
- Ortiz SCG (2010). Evaluación de la actividad antiproliferativa de las plantas *Struthanthus palmeri*, *Krameria erecta* y *Stegnosperma halimifolium* originarias de Sonora sobre las líneas celulares C3F6, L929, HELA y RAW. Departamento de Ciencias Químico-Biológicas. Hermosillo, Universidad de Sonora. PhD.
- Quideau S, Deffieux D, Douat-Casassus C and Pouységu L (2011). Plant Polyphenols: Chemical Properties, Biolo. Activities, and Synthesis." Angewandte Chemie International Edition 50(3):586-621.
- Ramírez SO, Córdova MM (2005). Evaluación de parámetros cinéticos para la *Saccharomyces cerevisiae* utilizando agua de coco como sustrato Ingeniería 15(1,2):91-102.
- Raven JA (1983). Phytophages of xylem and phloem: a comparison of animal and plant sap-feeders. Adv. Ecol. Res. 13:135-234.
- Rivero I (2010). Efecto hipoglucemiante de la planta *Cacalia decomposita* en ratones diabéticos-inducidos. Departamento de Ciencias Químico-Biológicas Hermosillo, Universidad de Sonora.

- PhD: pp.14-15.
- Rodriguez VJ, Vicente VO, Canteras MJ (1997). Valor del ensayo colorimétrico con MTT en el estudio del crecimiento y citotoxicidad *in vitro* de líneas de melanoma. *Patología* 30(1):18-27.
- Sakagami H, Kishimo K, Amano O, Kanda Y, Kuni S, Yokote Y, Oizumi H, Oizumi T (2009). Cell death induced by nutritional starvation in mouse macrophage-like RAW 264.7 cells. *Anticancer Res.* 29(1):343-348.
- Scudiero DA, Shoemaker, RH, Paull KD, Monks A, Tierney S, Nofziger TH, Currens MJ, Seniff D, Boyd MR (1988). Evaluation of a soluble tetrazolium/formazan assay for cell growth and drug sensitivity in culture using human and other tumor cell lines. *Cancer Res.* 48:4827-4833.
- Sramkoski RM, Pretlow TG, Giaconia JM, Schwartz S (1999). A new prostate carcinoma cell line, 22Rv1. *In Vitro Cell. Dev. Biol. Anim.* 35(7):403-409.
- Tezel TH, Del Priore LV, Kaplan HJ (2004). Reengineering of aged Bruch's membrane to enhance retinal pigment epithelium repopulation. *Investig. Ophthalm. Vis. Sci.* 45(9):3337-3348.
- Wataha JC, Hanks CT, Sun Z (1994). Effect of cell line on *in vitro* metal ion cytotoxicity. *Dent Matter* 10:156-61.